0013-7227/99/$03.00/0
Endocrinology

Vol. 140, No. 1
Printed in U.S.A.

Distinct Sites of Insulin-Like Growth Factor (IGF)-II Expression and Localization in Lesioned Rat Brain: Possible Roles of IGF Binding Proteins (IGFBPs) in the Mediation of IGF-II Activity*

H. J. WALTER, M. BERRY, D. J. HILL, S. CWYFAN-HUGHES, J. M. P. HOLLY, AND A. LOGAN

Department of Medicine (H.J.W., A.L.), University of Birmingham, Birmingham B15 2TT, United Kingdom; Department of Anatomy and Cell Biology (M.B.), UMDS, Guy's Hospital, London SE1 9RT, United Kingdom; Department of Medicine, Physiology and Paediatrics (D.J.H.), Lawson Research Institute, London, Ontario N6A 4V2, Canada; Department of Surgery (S.C.-H., J.M.P.H.), University of Bristol, Bristol, BS2 8HW, United Kingdom

ABSTRACT

Although expression of the IGF-II has been demonstrated within the central nervous system (CNS), past studies have failed to reveal its precise roles or responses subsequent to a traumatic injury. To demonstrate that IGF-II, IGFBP, and IGF receptor (-R) expression alters in response to a penetrating CNS injury, we used the techniques of ribonuclease protection assay, *in situ* hybridization, immunohistochemistry, Western blotting, and RIA. Under normal physiology, IGF-II expression is restricted to the mesenchymal support structures of the brain, including the choroid plexus, where its expression is coincident with that of IGFBP-2. Between 1–7 days post lesion (dpl), in the acute phase following a penetrant wound to the CNS, IGF-II and IGF-IIR protein, but not messenger RNA, were colocalized, with IGF-I, IGF-IR, and IGFBP-1, -2, -3, and -6, to neurons, macrophages, astrocytes, and microglia within the damaged tissue. Within the cerebrospinal fluid (CSF), levels of IGF-II peptide increased to peak at 7 dpl. IGFBP-2, -3, and -6 were also observed within the CSF, with IGFBP-2 predominating and exhibiting an increase in binding efficiency from 7–10 dpl. In the chronic phase of injury (7–14 dpl), an increase in both IGF-II, IGF-IIR and IGFBP-5 messenger RNA and protein was observed specifically and focally in the marginal astrocytes forming the limiting glial membrane of the wound. Thus, our evidence suggests that there are two mechanisms of action for IGF-II within the injured rat brain. During the acute phase, the secretion of IGF-II from the choroid plexus into the CSF is up-regulated, resulting in increased transport of the peptide to the wound. In the CSF, transported IGF-II is complexed to IGFBP-2 and essentially demonstrates an endocrine mode of action with a balance of locally produced IGFBPs modulating its bioactivity in the wound. Later in the wounding response, levels of IGF-II decline in the CSF and the wound neuropil, possibly with the aid of increased IGFBP-5 levels that may help to locally sequester and down-regulate IGF-II activity. Hence, in the chronic phase of the injury response, IGF-II reasserts itself to a predominantly autocrine/paracrine role restricted to the mesenchymal support structures, including the glia limitans, which may help reestablish and maintain tissue homeostasis. (*Endocrinology* **140:** 520–532, 1999)

AFTER injuries that penetrate the brain and spinal cord, damaged neurons that have survived the early autodestructive events begin to regrow during the acute phase of the wounding response (1–7 dpl). However, regeneration is aborted as a dense glial/fibrotic scar is laid down within the wound. Subsequent to the trauma, necrotic nervous tissue is phagocytosed, mostly by macrophages, which have been recruited into the lesion area from the blood, and also by activated glial cells. An influx of mesodermal cells from the meninges occurs between 4 and 10 dpl, depositing a matrix into the core of the lesion, around which an angiogenic response is now occurring. This dense fibrous scar, comprised of a matrix core surrounded by a glia limitans [an astrocyte/basal lamina membrane) that becomes contiguous with the glia limitans externa, contracts by 14 dpl providing a significant physical, and possible biochemical, barrier to axonal growth [see review by Logan *et al.* (1)]. Hence, although axons show a transient regenerative response, reconnection of severed neuronal pathways does not occur. It is postulated that many trophic factors regulate the wounding response, including IGF-II; however, their precise roles remain to be elucidated (1, 2).

In the CNS, IGF-II messenger RNA (mRNA) is detected from midgestation onwards (3), with significant levels of expression maintained in the leptomeninges, choroid plexus, and microvasculature after maturity, correlating with the sustained synthesis of immunoreactive IGF-II (4, 5). The peptide also becomes sequestered distal to these sites of synthesis within the myelin sheaths of individual axons and in nerve tracts (4). The significance of the distal depots of IGF-II peptide remains to be established; however, the spatial disparity between sites of synthesis and localization suggests that an effective mechanism of IGF-II translocation is operational. The CSF is possibly one transport route because, subsequent to secretion by the choroid plexus, it circulates

Received June 8, 1998.
Address all correspondence and requests for reprints to: Ann Logan, Department of Medicine, The University of Birmingham, Wolfson Research Laboratories, Queen Elizabeth Medical Centre, Edgbaston, Birmingham, B15 2TH, United Kingdom. E-mail: a.logan@bham.ac.uk.
* This work was supported by grants (to A.L. and M.B.) from The Wellcome Trust and The International Spinal Research Trust.

through the ventricles and ultimately into the subarachnoid space and its perivascular extensions, thereby infusing the whole brain (6). Samples of CSF from the subarachnoid space of intact mature brains contain IGF-II (7), implying that circulating CSF distributes IGF-II peptide, secreted from mesenchymal support structures, around the brain in a manner analogous to that of endocrine trophins. We suggest that just as hormones are secreted from a glandular epithelium into the systemic circulation, to affect receptor-bearing target cells distally, IGF-II is released from the choroid epithelium, into the CSF, and is then circulated to depots or distal targets.

IGF transport and bioactivity are regulated by a family of six high affinity binding proteins (IGFBP-1–6), which are complexed to the IGFs within the circulation and throughout the extracellular space [see reviews by Clemmons (8) and Jones and Clemmons (9)]. Within the intact CNS, IGFBP-2 and IGFBP-4, -5, and -6 mRNA expression have been demonstrated in the choroid plexus and meninges of the ventricular system, with IGFBP-2 predominating (4, 10–14). Small quantities of IGFBP-1 peptide have also been identified within the intact brain (10, 15). Under pathological conditions, IGFBP-2, IGFBP-3, and IGFBP-6 have been detected in CSF (16–19), suggesting that IGFBPs are involved in IGF-II transport from ventricular sites of synthesis to sites of storage and/or bioactivity.

IGF-II binds to specific, high affinity receptors (IGF-IR and IGF-IIR) that are expressed by a diverse range of cell types. IGF-IR mRNA is widely distributed in the CNS from early development and levels decline postnatally, although residual expression in (a) neurons of defined regions of gray matter (20–23); (b) glia of the white matter of the cerebral and cerebellar hemispheres, and brain stem, (24); (c) epithelial cells of the choroid plexi (10, 25–27); (d) ependyma of the third ventricle (10); and (e) brain capillary endothelial cells (10, 28) remains high. It is evident that most IGF-II activity is mediated via IGF-IR and its tyrosine kinase signalling pathway (29, 30). The suggestion that IGF-IIR may also mediate some actions through signaling pathways other than tyrosine kinases (31, 32) has not been substantiated. Nevertheless, IGF-IIR has a widespread distribution in the developing CNS (33) but, in the adult, is confined to specific neuronal perikarya, for instance, those of the pyramidal cell layer of the hippocampus and the granule cell layers of the dentate gyrus and cerebellar cortex (34, 35). Lower levels are also observed in the choroid plexus and meninges (34). By contrast to the distribution of detectable levels IGF-IIR mRNA, almost all neurons and astrocytes of the brain are IGF-IIR immunopositive (23, 36). While it is possible that these cells are expressing undetectable mRNA levels, it is also possible that the immunoreactivity detected represents soluble forms of the receptor that have been shed from distal sites of synthesis.

IGFs have neurotropic (37, 38) and gliogenic (39) activities *in vitro*. We hypothesize that, if IGF-II is involved in similar activities during the wounding response, then the expression of IGF-II mRNA and protein, together with IGFBPs and IGF-Rs, will alter in the traumatized CNS. Furthermore, if disparate sites of IGF-II synthesis and bioactivity are maintained in the injured brain, then acutely, we would predict an increase in IGF-II secretion by the choroid plexus and in titer within the CSF, with the peptide being transported to sites of bioactivity in the wound. This transportation would be facilitated by the increased production of specific potentiating IGFBPs, both at the sites of synthesis and bioactivity. Completion of the cellular responses would be associated with (a) a decline in IGF-II bioactivity within wounds, (b) reduction in expression of ligands/receptors/potentiating binding proteins, and (c) an enhancement in expression of inhibitory binding proteins. Therefore, the aims of this study were to localize and quantify the levels of IGF-II and IGF-IIR mRNAs and peptides within CNS wounds and the choroid plexus by ribonuclease protection assay (RPA), *in situ* hybridization, immunohistochemistry and additionally, to quantify the levels of IGF-II and IGFBP-1–6 peptide in the CSF by RIA and Western blotting, during the cellular wounding response using a rat model of penetrating brain injury. We have previously reported on the changes in expression of IGF-1, IGF-IR, and IGFBPs within CNS wounds in the same model (10).

Materials and Methods

Materials

These experiments employed radioisotopes, ECL detection kits, Hyperfilm MP and β-max film (Amersham International, Aylesbury, Buckinghamshire, UK); restriction endonucleases (Gibco BRL, Paisley, Scotland, or Promega Corp., Southampton, Hampshire., UK); modifying enzymes (Promega Corp.); nucleotides (Amersham Pharmacia Biotech, St. Albans, Hertfordshire, UK) and XL1-Blue bacteria (Stratagene, Cambridge, UK). All other reagents not specified were analytical grade from either Sigma Chemical Co. Ltd. (Poole, Dorset, UK) or BDH Merck Ltd. (Poole, Dorset, UK).

Plasmids for complementary RNA (cRNA) probe synthesis

The 662-bp coding region of mouse IGF-II (a modified transcript of one provided by V. Han, London, Ontario, Canada) is contained within the pGEM-4Z plasmid (Promega Corp.). *Hin*dIII and *Bgl*II were used to linearize the plasmid and SP6 and T7 were used to generate the transcript for antisense and sense templates respectively. The 500 bp rat IGF-IIR fragment (D. LeRoith, Bethesda, MD) is cloned within the pGEM-3 plasmid (Promega Corp.). *Eco*RI and *Xba*I were used to linearize the riboprobe, and T7 and SP6 generated the respective antisense and sense templates. Cyclophilin (J. Douglass, Oregon Health Science University of Medicine, Portland, OR) was an internal control in all ribonuclease protection assays to ensure equal loading on gels. The plasmid contains a 680 bp coding region of rat cyclophilin complementary DNA cloned within pSP65 (Promega Corp.). Cyclophilin has a ubiquitous tissue and phylogenetic distribution and represents 0.1–0.4% of total cytosolic protein in many mammalian tissues. It possesses strong homology to the enzyme peptidyl-prolyl cis-trans isomerase, which catalyses the slow cis-trans isomerization of proline peptide bonds in oligopeptides and accelerates slow, rate-limiting steps in the folding of several proteins in the cell. *Hin*dIII was used to linearize the plasmid for the antisense template. SP6 polymerase was used to generate the antisense cRNA probe.

Antibodies and recombinant proteins

All antibodies used were IgG fractions of rabbit polyclonals, except for IGFBP-5 (IgG fraction of an IGFBP-5 guinea pig polyclonal) and IGF-II (mouse IgG monoclonal). Antibodies not raised against rat proteins all have specified affinities for the corresponding rat ligand (see supplier's data sheet). Antihuman IGF-II antibody (Amano Biologicals, Troy, CA) cross-reacted <1% with IGF-I and antirat IGFBP-1 antibody (S. Shimasaki, San Diego, CA) had no known cross-reaction with other binding proteins. Antibovine IGFBP-2 antibody (Amano Biologicals) cross-reacted 0.1% with IGFBP-1, -3, -4, and -5, whereas antirat IGFBP-3

antibody (S. Shimasaki) cross-reacted with no other binding proteins, and antihuman IGFBP-4 antibody (TCS Biologicals Ltd., Botolph Claydon, Buckinghamshire, UK) had a cross-reactivity with IGFBP-1, -3, and -5 of 0.1–1% and up to 50% with IGFBP-2. Antihuman IGFBP-5 antibody (TCS Biologicals Ltd.) had a cross-reactivity with IGFBP-2 and IGFBP-3 of less than 1%, whereas antirat IGFBP-6 antibody (S. Shimasaki) cross-reacted with no other known binding proteins. Antirat IGF-IIR antibody (P. Nissley, Bethesda, MD) cross-reacted with neither IGF-IR nor the insulin receptor. Recombinant human (h)IGF-I, hIGFBP-1 and hIGFBP-3 for Western blotting were from TCS Biologicals Ltd. Recombinant hIGFBP-2, -4, -5, and -6 were purchased from Amano Biologicals. For RIA, recombinant hIGF-I and hIGF-II were purchased from GroPep Ltd. (Adelaide, Australia). All antibodies were usually stored at −20 C. If in frequent use, aliquots were stored at 4 C to prevent repetitive freeze/thawing. All recombinant proteins were stored at −70 C.

For immunohistochemistry. Antihuman IGF-II, IGFBP-4, and -5 antibodies were used at concentrations of 1:100, 1:3000, and 1:250 respectively, whereas antirat IGFBP-1, -3, -6, and IGF-IIR antibodies were used at 1:3500, 1:3000, 1:3500, and 1:2000, respectively. Antibovine IGFBP-2 antibody was used at the concentration of 1:3000.

For Western blotting. Antihuman IGFBP-4 and -5 antibodies were used at concentrations of 1:4000 and 1:1000, respectively, whereas antirat IGFBP-1, -3, and -6 were used at 1:4000. Additionally, antibovine IGFBP-2 and antirat IGF-IIR antibodies were used at the concentration of 1:4000 and 1:2000, respectively.

Animals and surgery

Surgery was performed aseptically under a British Government Home Office Licence. Groups of adult, female, 250 g Sprague Dawley rats were anesthetized ip with a mixture of Medetomidine (SmithKline Beecham, Welwyn Garden City, Hertfordshire, UK) at 100 μg/kg body weight and Ketamine hydrochloride (Parke-Davis Veterinary, Eastleigh, Hampshire, UK) at 10 mg/kg body weight or Hypnorm (fentanyl nitrate 0.134 mg/liter and fluanisone 10 mg/ml; Janssen Pharmaceuticals, Oxford, UK)/Hypnovel (midazolam 1 ml in 10 ml water; Roche, Welwyn Garden City, Hertfordshire, UK) at 8 ml/100 g body weight. Buprenorphine (Sterling Health, Guildford, Surrey, UK) was administered postoperatively as an analgesic. After craniotomy, the mediolateral right cerebral cortex was incised using a David Kopf (Charles River, Margate, Kent, UK) stereotactic instrument. The lesion was made precisely to a depth of 4 mm along a 4.5 mm line parallel with the sagittal suture, 3 mm lateral to the mid-line, and spanning the fronto-parietal suture. Animals were allowed to recover post surgery for periods of 0, 2, 5, 7, and 15 dpl and fed *ad libitum*.

Sampling of CSF

Under deep anesthesia, an incision was made in the suboccipital skin. The occipital semispinalis and trapezius muscles were separated in the mid-line to expose the posterior atlanto-occipital membrane. A Hamilton syringe needle was inserted through the membrane into the cysterna magna and CSF withdrawn, samples from four animals were pooled and frozen rapidly in liquid nitrogen and stored at −70 C until processed.

Histology

Groups of four animals were deeply anesthetized (as for surgery) and perfused transcardially with 250 ml of saline followed by 250 ml of 4% paraformaldehyde (PFA) in saline. Following excision, brains were post-fixed overnight in 4% PFA (wt/vol, in 0.1 M sodium tetraborate) at 4 C, dehydrated in graded alcohols, embedded in low melting point polyester wax (40), and stored at −70 C. Sections, 7 μm thick, were cut through the lesion site using a microtome (Bright, Huntingdon, Cambridgeshire, UK) fitted with a cooled chuck, and mounted on slides coated with either a 1% gelatin solution (for immunohistochemistry), or with Biobond (British Biocell Int., Cardiff, Glamorgan, UK; for *in situ* hybridization). Once mounted, sections were air dried and stored at either −70 C (*in situ* hybridization) or at 4 C (immunohistochemistry).

RNA extraction

Groups of three rats were killed with an anesthetic overdose, the brains removed, rapidly dissected on ice, and stored at −70 C until extraction. Total cellular RNA was extracted from the lesioned and unlesioned hemispheres of the brain, using the RNAzol B method (Biogenesis, Bournemouth, Dorset, UK), a modification of the single-step method (41). Briefly, frozen tissue was weighed and homogenized in 2 ml RNAzol per 100 mg tissue. Chloroform was added (0.2 ml/2 ml) and shaken for 15 sec before placing on ice for 5 min. Samples were centrifuged at 5000 × *g* for 20 min at 4 C (Dupont Sorvall RC5C, SS34 rotor, High Wycombe, Buckinghamshire, UK). The aqueous phase was removed and precipitated with an equal volume of isopropanol for 15 min on ice. Samples were centrifuged as above, washed with 75% ethanol and redissolved in 200 μl ultrapure water. RNA was quantified by optical density at 260 nm and 280 nm and checked for integrity on a 1% agarose gel.

Radioactive probe synthesis

cRNA probes for ribonuclease assay. Transcription buffer [40 mM Tris, pH 7.5, 6 mM $MgCl_2$, 2 mM spermidine and 10 mM sodium chloride (NaCl)], 20 U rRNasin, 10 mM dithiothreitol (DTT), 0.5 mM ATP, GTP, UTP, 12 μM CTP (150 μM for cyclophilin), 0.5 μg linearized antisense plasmid, 50 μCi ^{32}P CTP (5 μCi for cyclophilin) and 15 U RNA polymerase were incubated together at 37 C for 1 h. DNase I (1 U) was added and the reaction left at 37 C for a further 15 min. Yeast transfer (t)RNA (20 μg) was added before a phenol:chloroform/chloroform extraction and ethanol precipitation. The cRNA probe was washed with 75% ethanol, briefly dried, and resuspended in ultrapure water. The probe, 1 μl in 5 ml Ecolite+ scintillation fluid (ICN flow, High Wycombe, Buckinghamshire, UK), was counted using a Pharmacia counter for 60 sec. ^{32}P-labeled cRNA probes were stored at −20 C for no longer than 1 week.

cRNA probes for in situ hybridization. Transcription buffer, 20 U rRNasin, 10 mM DTT, 2 mM ATP, GTP, CTP, 0.5 μg linearized antisense or sense plasmid, 200 μCi ^{35}S UTP, and 15 U RNA polymerase were incubated together at 37 C for 2 h. DNase I (1 U) was added, and the reaction left at 37 C for a further 15 min. To the reaction mix, 60 mM EDTA pH 8.0 was added to a final volume of 50 μl, and loaded onto a Sephadex G50 Quick Spin column (Boehringer Mannheim, Lewes, E. Sussex, UK) which was centrifuged at 1100 × *g* (Hereaus Sepatech Varifuge 3.2RS, Brentwood, Essex, UK) for 4 min. DTT was added to a final concentration of 150 mM. The probe, 1 μl in 5 ml Ecolite+ scintillation fluid, was counted for 60 sec. ^{35}S-labeled cRNA probes were stored at −20 C and kept for approximately 2 weeks. Before use, the ^{35}S-labeled cRNA probes were recounted and their integrity checked on a 4% polyacrylamide/8 M urea gel.

^{125}I labeling of IGF-I/IGF-II. Recombinant hIGF-I and hIGF-II were labeled with ^{125}I using the chloramine-T method (42) under appropriate safety conditions. The fractions were collected in 0.5 ml aliquots and 1 μl of each was counted on a γ counter to locate the protein peak (LKB-Pharmacia). The radiolabeled protein fractions were stored at −20 C until required.

Ribonuclease protection assay

RPAs were performed on total RNA extracted from the cerebral hemispheres of three rats from each treatment group. Total RNA (20 μg) was dissolved in 30 μl of hybridization solution (80% formamide, 40 mM PIPES, pH 6.4, 400 mM NaCl and 1 mM EDTA, pH 8.0) containing 60,000 cpm and 20,000 cpm of an IGF-related and cyclophilin ^{32}P-labeled cRNA probe. After being heated to 85 C for 5 min, the cRNA probe was allowed to anneal the endogenous RNA at 45 C overnight. At the end of the hybridization, the solution was diluted with 350 μl of RNase digestion buffer (300 mM NaCl, 10 mM Tris, pH 7.4, and EDTA, pH 7.5), containing 40 μg/ml of RNase A and 500 U/ml of RNase T1, and incubated for 1 h at 30 C. Proteinase K (100 μg) in 10% SDS was added to the sample and the mixture incubated at 37 C for an additional 20 min. Following a phenol:chloroform extraction and ethanol precipitation, the pellet containing the RNA:RNA hybrid was briefly dried and resuspended in loading buffer (80% formamide, 0.1% xylene cyanol, 0.1% bromophenol blue and 2 mM EDTA, pH 8.0). The samples were boiled at 90 C for 5

min and separated on a 4% polyacrylamide/8 M urea gel. ^{32}P end-labeled (DNA polymerase 1) *Hin*fI digested pBR322 fragments were used as molecular markers. The mRNA protected fragments were visualized by autoradiography against Amersham Hyperfilm MP (Amersham International) at −70 C.

In situ hybridization

Mounted sections were dewaxed in ethanol, rehydrated, washed, and digested with 10 μg/ml proteinase K in 0.1 M Tris containing 50 mM EDTA at 37 C for 30 min. Sections were rinsed in deionized water followed by an incubation in 0.1 M triethanolamine (TEA), pH 8.0, for 3 min. Sections were then acetylated for 10 min with 0.25% acetic anhydride in 0.1 M TEA for 10 min, rinsed in 2 × SSC, dehydrated through a graded series of ethanol washes, and air dried under vacuum for 2 h before hybridization. Hybridization with the ^{35}S-labeled cRNA probe (1×10^7 cpm/ml) was performed at 55 C overnight in 10 mM Tris, pH 8.0, containing 50% formamide, 0.3 M NaCl, 1 mM EDTA, pH 8.0, 0.02% polyvinylpyrrolidone, 0.02% Ficoll, 0.02% BSA, 10 mM DTT, 0.05 mg/ml torula yeast RNA (C. P. Laboratories, Bishops Stortford, Hertfordshire, UK), 0.5 μg/ml tRNA and 10% dextran sulfate (wt/vol). After hybridization, sections were rinsed for 1 h in 4 × SSC and treated with 25 μg/ml RNase A in 10 mM Tris, pH 8.0, containing 0.5 M NaCl and 1 mM EDTA pH 8.0 at 37 C for 30 min. This was followed by increasing high stringency washes of SSC containing 1 mM DTT, finishing with 0.1 × SSC at 65 C for 30 min. Slides were then dehydrated through a graded series of ethanol, dried under vacuum, and then exposed to Hyperfilm β-max film for 10 days at 4 C to examine gross changes in mRNA. For microscopic analysis, slides were exposed to Ilford K5 liquid autoradiographic emulsion (Ilford Ltd., Basildon, Essex, UK) for 2 weeks at 4 C, processed with Kodak D19 developer (Eastman Kodak, Rochester, NY), rinsed and fixed with Kodak rapid fixer. The slides were rinsed for 30 min in tap water, counterstained with Mayer's haemalum, examined by darkfield and brightfield microscopy using a Zeiss Axioscope microscope [Carl Zeiss (Oberkochen) Ltd., Welwyn Garden City, Hertfordshire, UK], and photographed using Ilford PanF ISO 50 black and white film.

Immunohistochemistry

For immunoperoxidase staining (ABC Vectastain Elite kit, Vector Laboratories, Inc., Peterborough, Cambridgeshire, UK), tissue sections were dewaxed in 100% ethanol for 5 min and then rehydrated in 5-min steps in descending concentrations of ethanol to ultra-pure water. Subsequent to a 5 min equilibration in PBS, the endogenous peroxidase was quenched by incubating with 0.01% hydrogen peroxide (H_2O_2) in PBS for 30 min. The sections were rinsed in PBS and incubated in 1.5% goat serum (vol/vol, Vector Laboratories, Inc.) diluted in PBS containing 0.1% BSA for 30 min to block nonspecific staining.

After an overnight incubation at 4 C, with the appropriate concentration of growth factor, binding protein or receptor-protein-A-purified primary antibody diluted in PBS supplemented with 5% BSA, most sections were treated with a 1:200 dilution of biotinylated goat antirabbit IgG for 1 h, except for the IGFBP-5 antibody treated sections for which biotinylated antiguinea pig IgG and for IGF-II, for which biotinylated antimouse IgG were used. This was followed by 1 h incubation with the Vectastain Elite ABC reagent (Vector Laboratories, Inc.), a biotin-avidin-peroxidase complex. Finally, the sections were treated for 2–7 min with 0.5 mg/ml 3′3′-diaminobenzidine in PBS containing 0.01% H_2O_2. All steps were separated by PBS buffer washes. The sections were washed in PBS, counterstained with Mayer's haemalum, dehydrated, and, after being cleared and mounted, examined by brightfield microscopy under differential interference contrast (DIC) optics, on a Zeiss Axioscope microscope and photographed using Fujicolor Super G plus ISO 200 color film (Fuji Photo Film Co., Ltd., Tokyo, Japan).

The specificity of the antibodies was verified by preincubating the primary antibody with excess (>1 μg) of the appropriate homologous or heterologous antigenic growth factor/binding protein. Sections were also processed with the primary or secondary antibody omitted. All of these controls yielded no visible staining of the sections. Antibodies to each binding protein were preincubated with every other recombinant binding protein species to determine specificity of staining.

Western blotting

CSF (2.5 μl or 10 μl from pooled samples from four animals) was diluted with 97% sample buffer (0.16 M Tris HCl, pH 6.8, 22% glycerol, 6.1% SDS, 0.02% bromophenol blue, 0.02% xylene cyanol). Rainbow colored (10 μl; Amersham International) and unstained, low (and where appropriate high) molecular weight molecular markers (37.5 μg; LMW electrophoresis calibration kit, Pharmacia) and normal rat serum were diluted with 95%, 100% and 97% sample buffer, respectively. Samples were heated to 100 C for 5 min and immediately loaded onto a 0.1% SDS/12.5% polyacrylamide reducing gel. The separated protein components were electroblotted in transfer buffer (0.1 M Tris, 0.57 M glycine, 20% methanol (vol/vol), pH 8.3) onto a Hybond C super (Amersham International) nitrocellulose membrane using an LKB electroblotting unit (Pharmacia). A current of 0.8–1.0 A was applied for 4 h at 4 C (or where appropriate overnight). The membranes were air dried for 10–15 min. The marker lanes were removed from the membrane and stained with amido black solution (0.1% amido black, 7% acetic acid, 25% methanol) and then destained (10% acetic acid, 25% methanol) until the background of the filter was white.

Membranes were incubated in Nonidet P-40 solution (5 mM Tris HCl, 0.05% Nonidet P-40, pH 7.4) for 30 min, BSA solution (5 mM Tris HCl, 3% BSA, pH 7.4) for 30 min, Tween 20 solution (5 mM Tris HCl, 15 mM NaCl, 0.2% Tween 20, pH 7.4) for 20 min, before being air dried. Radioactive (^{125}I) IGF-I/IGF-II tracer at 10,000–16,000 cpm/100 μl was added to BSA solution and incubated with the membrane for 2 h. After discarding the radioactive probe, the membrane was washed in Tween 20 wash solution (50 mM Tris HCl, 0.15 M NaCl, 0.4% Tween 20, pH 7.4) for 15 min. This was followed by three washes of 15 min in Tris-buffered saline (50 mM Tris HCl, 0.15 M NaCl, pH 7.4). Membranes were air dried, covered in Saran wrap, and exposed to Kodak X-OMAT LS film at −80 C for 2–3 days. The film was processed in Kodak GBX developer, replenisher, and fixer.

The membranes were then blocked by shaking for at least 2 h in TBSTM (5% dried milk powder (Marvel, Premier Beverages, Stafford, Staffordshire, UK), dissolved in 15 mM Tris base, 0.22 M NaCl, 0.2% Tween 20, pH 7.4). During this time, the TBSTM was changed at least once. Membranes were placed in 10 ml/blot of primary antibody diluted in TBSTM, and rotated overnight. After two 30-min washes in TBSTM and one for 30 min in TBST, secondary antibodies were added. Antibodies were diluted to a final volume of 10 ml (antirabbit IgG-peroxidase 1:10000, antiguinea pig IgG-peroxidase 1:500) and placed with the membranes for 1 h. Membranes were washed three times for 15 min in TBST, followed by a brief rinse in ultra-pure water. An equal volume of Luminol (ECL detection kit; Amersham International) reagent 2 followed by Luminol reagent 1 was added. The solution was uniformly exposed to the membranes for 70 sec. All the Luminol reagents were removed, the membranes sealed in a plastic bag and placed immediately against Kodak X-OMAT LS film. The membranes were exposed against the film for approximately 1 h. Films were processed in Kodak GBX developer and replenisher.

RIA

IGF-II was measured in pooled samples of CSF from 4 rats by specific RIA, as previously described (43) following removal of IGFBPs by gel filtration chromatography on Sephadex G75 and elution with 1 M acetic acid. The following modifications were employed from the published methods. The primary antiserum was a rabbit antihuman IGF-II antibody (GroPep) and was used at a final concentration of 1:1250. Recombinant hIGF-II (GroPep) was used as the iodinated ligand for the standard curve (0.16 ng/ml to 20 ng/ml). Incubation with the primary antiserum was for 3 days before centrifugal separation of the bound and free tracer following the addition of PEG-8000. The minimum level of detection of IGF-II was 0.6 ng/ml, cross-reactivity with IGF-I was less than 1%, and the intra and interassay coefficients of variation were 8% and 13%, respectively. The recovery of IGF-II following gel chromatography was estimated as greater than 90% as measured with the radiolabeled IGF-II added to biological samples.

Densitometric and statistical analysis

Autoradiographic gels were scanned using a ScanJet IIc and Deskscan II software (both from Hewlett-Packard Co., Geneva, Switzerland) into

a Macintosh LC475 computer (Apple Computer Inc., Cupertino, CA). On RPA autoradiographs, bands corresponding to the protected mRNA fragments of IGFs, IGFBPs, IGF-Rs and cyclophilin, were densitometrically quantified into arbitrary units using NIH Image analysis software (NIH). The IGF-related bands of interest were normalized by dividing IGF-related mRNA pixel values by cyclophilin mRNA values. Likewise, similar quantifications were performed on Western blot autoradiographs, on bands indicating IGF-ligand or IGFBP-antibody binding. Where appropriate, both means and SEM were calculated and plotted. Significant differences in relation to data from either the 0 dpl control, or the contralateral unlesioned hemisphere, were examined using single-factor ANOVA with a significance (α) level of 5%.

TABLE 1. Localization of IGF-II and IGF-IIR mRNA and protein in the intact and lesioned cerebral hemisphere visualized by *in situ* hybridization and immunohistochemistry

	IGF-II		IGF-IIR	
	mRNA	Protein	mRNA	Protein
INTACT				
Choroid	++	++	++	++
Meninges	++	++	++	++
Ependyma	−	++	−	++
White matter	−	++	−	++
Cortical neurons	−	−	−	−
Cortical astrocytes	−	−	−	+
WOUND				
Neurons	−	++	−	++
Astrocytes of the glia limitans	++	++	++	++
Macrophages	−	++	−	++
Microglia	−	++	−	++
Endothelium	++	++	−	++
RESPONSE PEAK	5–12 dpl		2–5 dpl and 12 dpl	

++, Present; +, low levels present; −, absent levels; dpl, days post lesion.

Results

The post injury temporal distributions of IGF-II and IGF-IIR mRNA and protein within a penetrant wound of the cerebral hemisphere and IGF-II and IGFBP-1–6 protein within the CSF are summarized in Tables 1 and 2, respectively. All data mentioned, but not present herein, are available for inspection on written request to the corresponding author. The localization of IGF-I, IGFBP-1–6, and IGF-IR mRNA and peptide, in unlesioned and lesioned adult rat brains, has been catalogued by us in detail elsewhere (10), as has the localization of IGF-II throughout the intact brain (4). IGF-II and IGF-IIR mRNA and peptide expression altered in response to injury, as did corresponding levels of IGF-II peptide within the CSF. IGFBP-2, -3, and -6 peptides were also observed within the CSF. Here, levels of IGFBP-2 predominated and were injury responsive. Because the corresponding IGF-II and IGFBP mRNAs were expressed in the choroid plexus, this site was a likely source of these proteins. No IGF-I, IGFBP-1, IGFBP-4, or IGFBP-5 peptide were detected in the CSF by the methods described here.

TABLE 2. Presence of IGF-I, IGF-II, IGFBPs, and IGF-IIR protein in the CSF of the injured adult rat brain detected by Western ligand and immunoblotting

	RIA		Western blotting									
	IGF-I	IGF-II	IGFBP-1	IGFBP-2		IGFBP-3		IGFBP-4	IGFBP-5	IGFBP-6		IGF-IIR
				Ligand	Immuno	Ligand	Immuno			Ligand	Immuno	Immuno
CSF	−	++	−	++	++	++	++	−	−	+	++	−
Response peak	N/A	7 dpl	N/A	7–10 dpl	7–10 dpl	2 & 15 dpl	2 dpl	N/A	5–7 dpl	N/Q	2 dpl	N/A

++, Present; +, low levels present; −, absent levels; dpl, days post lesion; N/A, not applicable; N/Q, not quantifiable.

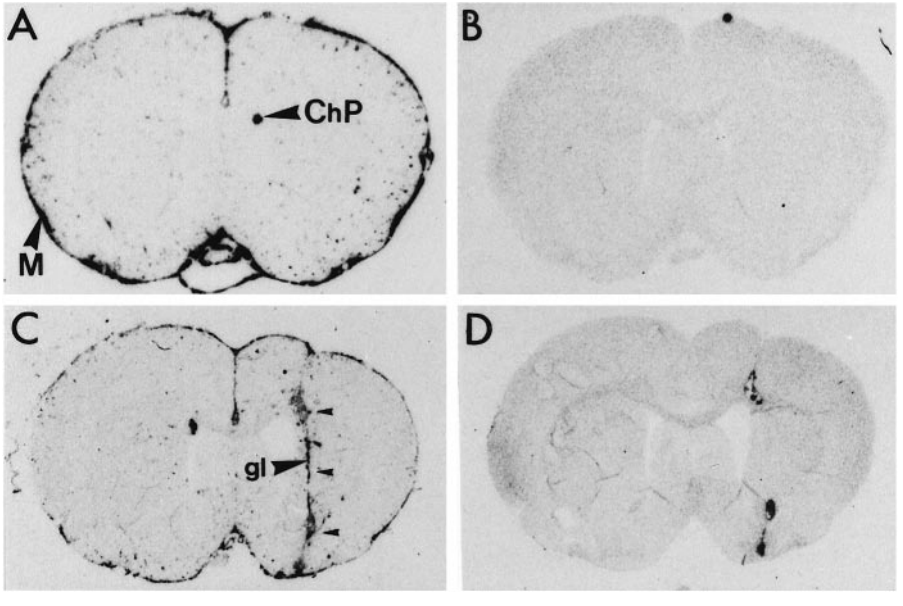

FIG. 1. Autoradiographic macroscopic visualization of IGF-II mRNA, by *in situ* hybridization, in brains. A, Intact brain, IGF-II antisense hybridized; B, intact brain, IGF-II sense hybridized; C, lesioned brain at 12 dpl, IGF-II antisense hybridized; D, lesioned brain at 12 dpl, IGF-II sense hybridized. Nonspecific binding, of the sense cRNA probe, to the hematogenous core of the wound is visible (compare C and D). ChP, Choroid plexus; M, Meninges; gl, glia limitans; *small arrows* depict the lesion path.

IGF-II in the cerebral hemisphere

A 662-bp protected mRNA species was identified by RPA, both in unlesioned and contralateral lesioned cerebral hemispheres, corresponding to IGF-II mRNA. By RPA, which is a relatively insensitive method, no significant differences in total mRNA signal were detected in the lesioned hemisphere compared with either the contralateral unlesioned hemisphere at any time point or the 0 d control animals (data not shown). By *in situ* hybridization, high levels of IGF-II mRNA were focally localized throughout the meninges and the ventricular choroid plexi of the intact and lesioned brains, and also later within the developing wound glia limitans (Figs. 1 and 2). In the acute phase (1–7 dpl), IGF-II mRNA levels did not increase within any cells of the damaged neuropil, whereas in the chronic phase mRNA expression was strong and specifically localized within the marginal astrocytes of the forming glia limitans of the scar (Figs. 1C and 2, G–H).

By contrast, IGF-II immunoreactivity was observed in the neuropil around the wound in the injured cerebral hemisphere at all time points, but most obviously in the acute phase at 5 dpl and was localized to neurons, macrophages, astrocytes, and microglia (Fig. 3, A and B). Additionally, after 7 dpl, most of the astrocytes of the forming glia limitans became strongly IGF-II immunoreactive (Fig. 3C). Additionally, IGF-II peptide was also detected within CSF samples by RIA. Low levels of IGF-II were present within CSF samples from unlesioned brains, with the levels increasing transiently post injury to peak at 7 dpl (Fig. 4).

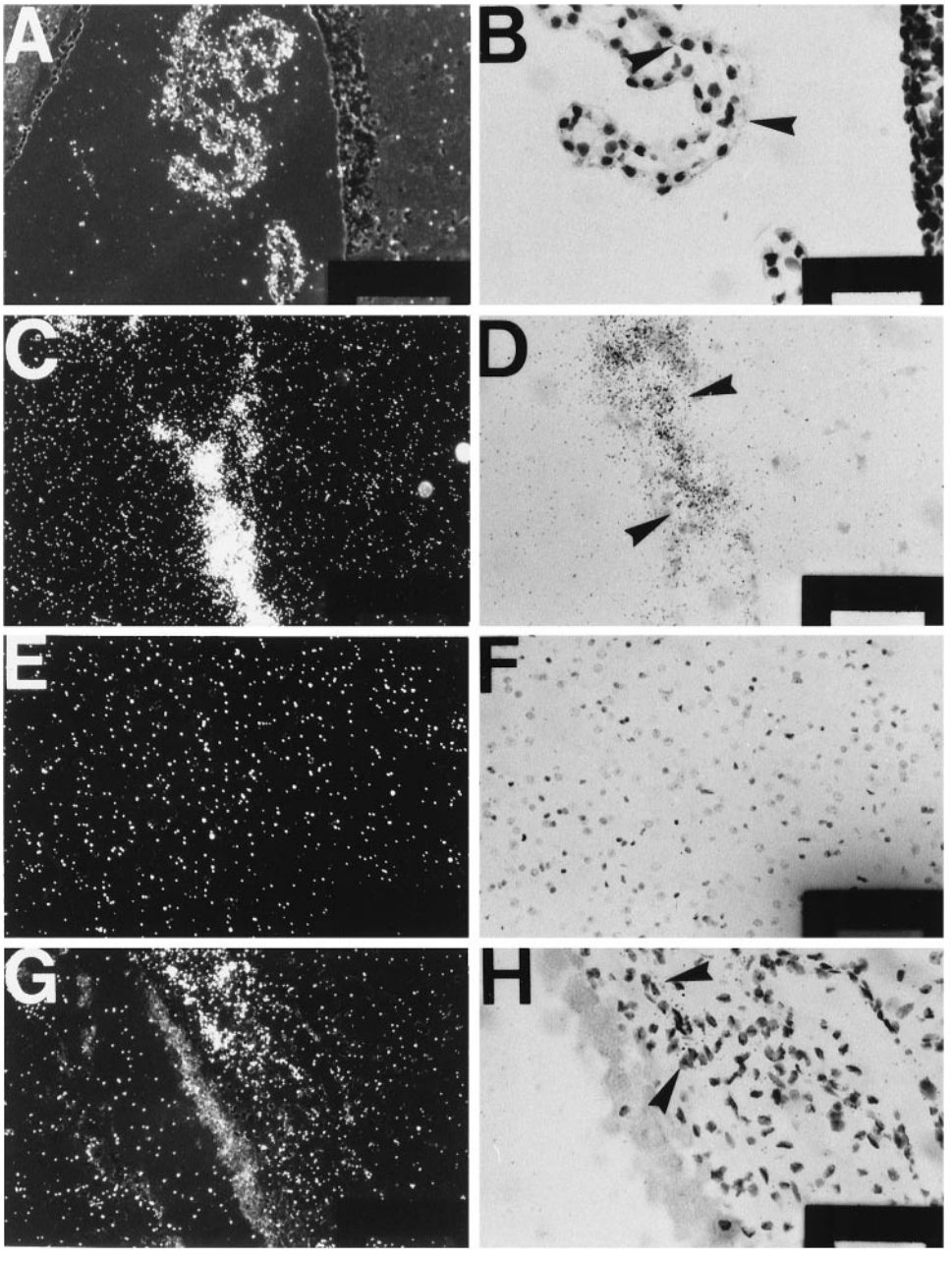

FIG. 2. Microscopic darkfield (DF) and brightfield (BF) visualization of IGF-II mRNA, by *in situ* hybridization, in brains. *Arrows* indicate areas of positive hybridization. A, Choroid plexus, intact brain (DF); B, choroid plexus, intact brain (BF); C, meninges, intact brain (DF); D, meninges, intact brain (BF); E, unlesioned cerebral cortex at 12 dpl (DF); F, unlesioned cerebral cortex at 12 dpl (BF); G, lesioned cerebral cortex at 12 dpl, taken from the lesion path (DF); H, lesioned cerebral cortex at 12 dpl, taken from the lesion path (BF). *Bar*, 10 μm (DF) and 5 μm (BF).

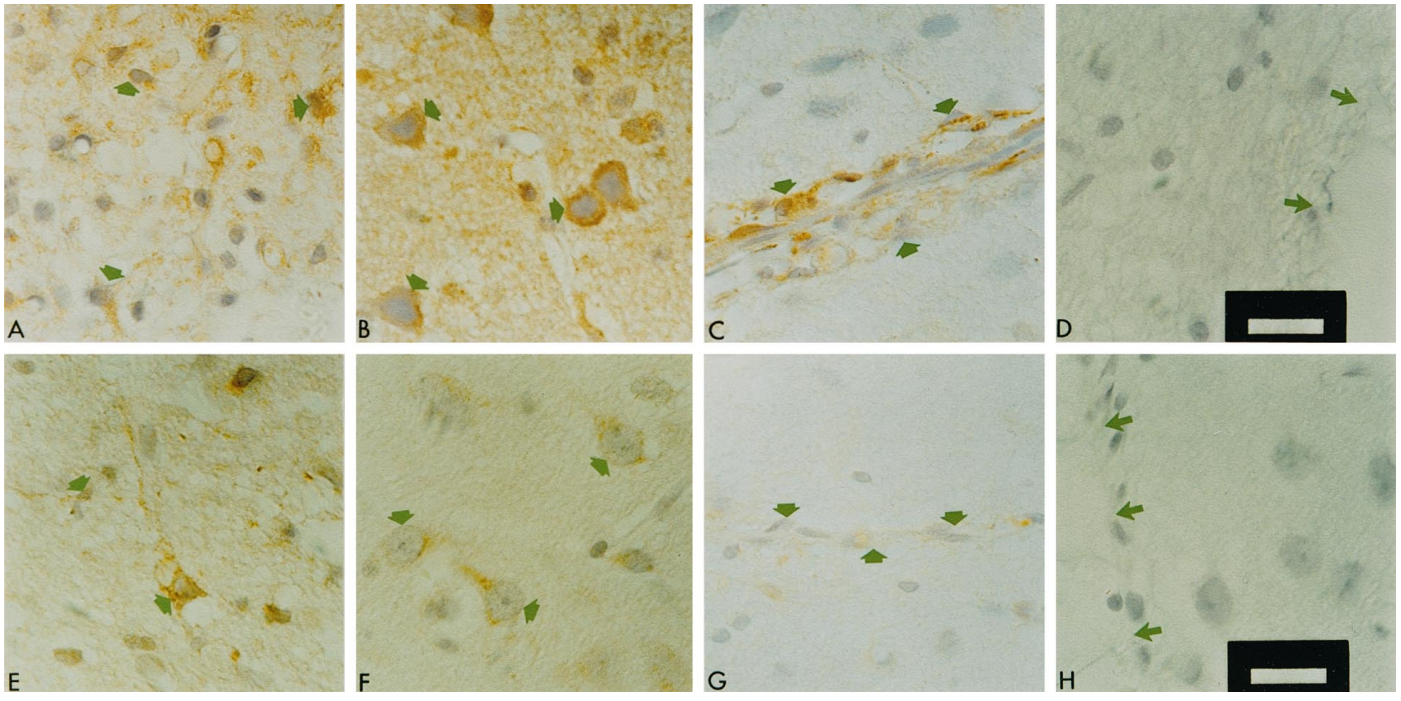

FIG. 3. Cellular localization of immunoreactive IGF-II and IGF-IIR peptide in lesioned cerebral hemispheres at 12 dpl. Brightfield micrographs taken under oil immersion using DIC optics are shown. IGF-II in A, astrocytes (*arrowed*); B, neurons (*arrowed*); C, astrocytes of the wound's glia limitans (*arrowed*); D, preabsorbed IGF-II antibody control (*arrows* show lesion course); and IGF-IIR in E, astrocytes (*arrowed*); F, neurons (*arrowed*); G, astrocytes of the wound's glia limitans (*arrowed*); H, IGF-IIR antibody omission lesion control (*arrows* show lesion course). *Bar*, 2 μm.

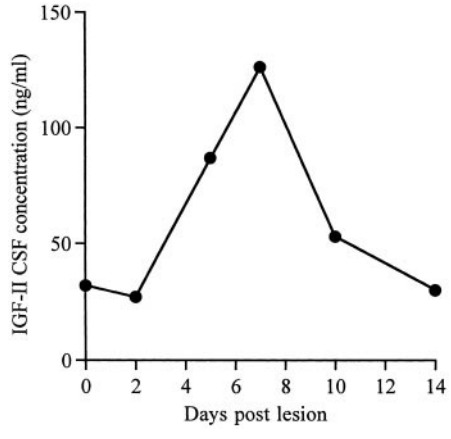

FIG. 4. RIA of CSF for the detection of IGF-II. CSF samples were taken from the cysterna magna of 4 rats at 0, 2, 5, 7, 10, and 14 days post cerebral lesion, pooled and IGF-II titres measured by specific RIA (expressed as ng/ml CSF).

Western ligand blotting of IGFBPs in CSF

Four bands were detected in pooled samples of CSF from brains at various times between 0 d and 14 d post lesion (Fig. 5A). A predominant probable IGFBP-2 band was observed at approximately 30 kDa, with two lesser bands between 39–43 kDa, which may have been IGFBP-3, and a faint band at 20 kDa (possibly IGFBP-6) that was unquantifiable (n = 2).

When lower quantities of the same CSF samples were analyzed to enhance visualization of the IGFBP-2 band, the ligand binding efficiency of the 30 kDa band was seen to be significantly increased in the CSF between 6–10 dpl (n = 7, F > Fcrit at the 5% level; Table 3) compared with the 0 d control (Fig. 6, A and B). The response was transient, peaking at 7–10 dpl and declining thereafter. A small biphasic increase in ligand binding was also observed in the CSF in the 39–43 kDa bands with peaks at 2 and 15 dpl compared with the 0 d. (Fig. 5B).

Western immunoblotting of IGFBPs in CSF

IGFBP-2. Immunoblotting with IGFBP-2 antibodies showed two IGF-related peptides, one at approximately 32 kDa, the other at approximately 18 kDa (Fig. 7A) in the CSF from intact as well as lesioned brains. The 32-kDa band followed a similar pattern of increase to that of the 30 kDa protein on the ligand blot, suggesting that this was intact IGFBP-2. The levels of this BP increased from 2 dpl to peak between 7–10 dpl and thereafter declined (Fig. 7B). The smaller 18 kDa peptide, which did not bind ligand and probably represents a residual fragment of proteolytically cleaved IGFBP-2, showed a sustained increase in expression during the full time course of the experiment (Fig. 7B).

IGFBP-3

Western immunoblot analysis of CSF with IGFBP-3 antibodies (data not presented) showed that immunoreactive IGFBP-3 protein increased in the CSF at 2 dpl, with levels following a similar pattern to those displayed by the 39–43 kDa protein on the ligand blot (Fig. 5B).

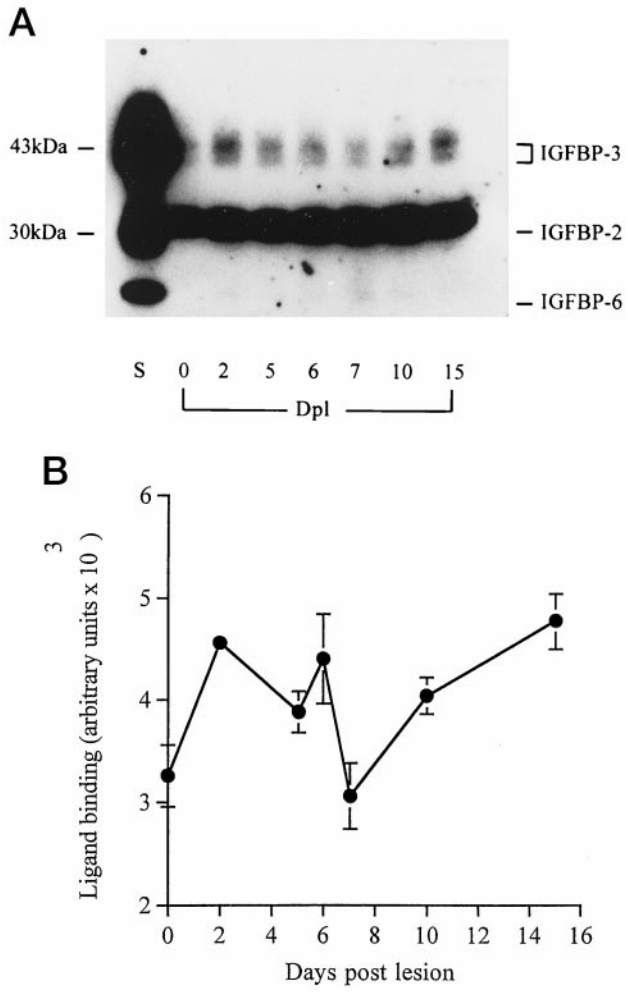

FIG. 5. Western ligand blotting for the determination of the presence of all detectable IGFBPs within CSF. Three major species of IGFBP are visible, which may correspond to IGFBP-3, IGFBP-2, and IGFBP-6. A, Western ligand blot loaded with 10 μl CSF; B, relative ligand binding values of the 39–43 kDa, IGFBP-3 bands. Means and SEM are shown (n = 2). S, Normal serum; Dpl, days post lesion.

IGFBP-6

Using IGFBP-6 antibodies, one band was visible at approximately 23 kDa, probably corresponding to the 20-kDa protein band observed on the ligand blot. Titers of immunoreactive IGFBP-6 protein showed a small increase at 2 dpl, but values subsequently declined and by 10 dpl levels equivalent to those observed in the 0 d control sample were recorded (data not shown).

IGF-II receptor in the cerebral hemispheres

A 500-bp protected mRNA species corresponding to IGF-IIR was identified by RPA in all samples. There were no significant changes in mRNA expression in any of the unlesioned or lesioned hemispheres when examined by RPA (data not shown). By *in situ* hybridization, low levels of IGF-IIR mRNA were detected diffusely throughout the brain (Fig. 8), barely above background, with high levels of expression localized to the piriform cortex, internal capsule, meninges and ventricular choroid plexi, in both the intact and lesioned brain (Fig. 9, A–D). Within the wound, changes in IGF-IIR mRNA in response to injury were identified, but the response was strictly localized to the astrocytes of the maturing glia limitans and only became apparent at 12 dpl (Fig. 9, G–H).

In intact cerebral hemispheres, immunoreactive IGF-IIR peptide was detected in the ependyma, blood vessels, meninges, choroid plexus, and all myelinated nerve tracts. Most, if not all, neurons were weakly immunopositive with many neuronal subpopulations exhibiting strong immunoreactivity, including those of the piriform cortex and supraoptic nuclei. Immunopositive astrocytes, microglia, macrophages and neurons were also observed in wounds after lesioning. At 2 dpl, strong immunopositive staining was apparent in neurons, microglia and astrocytes around the wound, with immunopositive macrophages appearing by 5 dpl. The response in the neuropil declined between 7–10 dpl to reveal residual staining in astrocytes and neurons (Fig. 3, E and F), although immunopositive IGF-IIR staining appeared at 12 dpl to be associated with the astrocytes comprising the maturing glia limitans (Fig. 3G).

Discussion

The distribution of IGF-II mRNA and protein within the adult rat brain is distinct from that of IGF-I, both before and after injury. After a penetrating cerebral injury, spatio-temporal changes in IGF-II expression and localization occurred within the damaged CNS. The accompanying altered pattern of expression of specific IGFBPs and IGF-Rs, implicates IGF-II in CNS wound healing as an endocrine regulator of cellular responses.

In our previous description of the normal distribution of IGF-II in the adult rat brain (4), IGF-II mRNA was seen to be expressed in the highly vascularized areas of the mesenchymal support structures, predominantly in the meninges, microvasculature, and the ventricular choroid plexi. Additional levels of high expression were also observed within the hippocampus and thalamus. Colocalized IGF-II peptide in areas of high mRNA expression, indicated mRNA translation (4). Thus, IGF-II expression was, in part, associated with structures that are involved in the production of extracellular fluids (including CSF), which are responsible for substrate transport and supply in the CNS (4, 5). The presence of IGF-II protein in CSF has previously been demonstrated, together with a number of putative transport proteins (44). The coexpression of IGFBP-2 by cells of the choroid plexus and meninges and the corresponding detection of significant levels of IGFBP-2 peptide coincident with IGF-II within the CSF (4, 18, 45, 46) adds weight to the hypothesis that IGFBP-2 is a key transport protein for IGF-II in the CNS, mediating its transfer via the CSF from sites of synthesis to sites of storage and/or bioactivity. Certainly, this hypothesis would explain the localization of immunoreactive IGF-II and IGFBP-2 in the absence of significant levels of their mRNA at sites throughout the brain (4). Furthermore, this pattern of differential siting of IGF-II expression and bio-

TABLE 3. ANOVA of the 30-kDa band in Western ligand blots

Sources of variation	0 dpl	6 dpl	0 dpl	7 dpl	0 dpl	10 dpl
Sum	2978	5394	2978	7433	2978	7453
Average	425.43	770.57	425.43	1061.9	425.43	1064.7
Variance	7E+04	8E+04	7E+04	8E+04	7E+04	1E+05
SS:	Between groups		4.2E+05	1.4E+06		1.4E+06
	Within groups		9.2E+05	8.7E+05		1.1E+06
	Total		1.3E+06	2.3E+06		2.5E+06
df:	Between groups		1	1		1
	Within groups		12	12		12
	Total		13	13		13
MS:	Between groups		4.2E+05	1.4E+06		1.4E+06
	Within groups		76652	72054		91392
	F		5.439	19.675		15.651
	P value		0.038	0.001		0.002
	F crit		4.747	4.747		4.747
	F>Fcrit		5% level	5% level		5% level

Data were analyzed using single-factor ANOVA with an α of 5%.

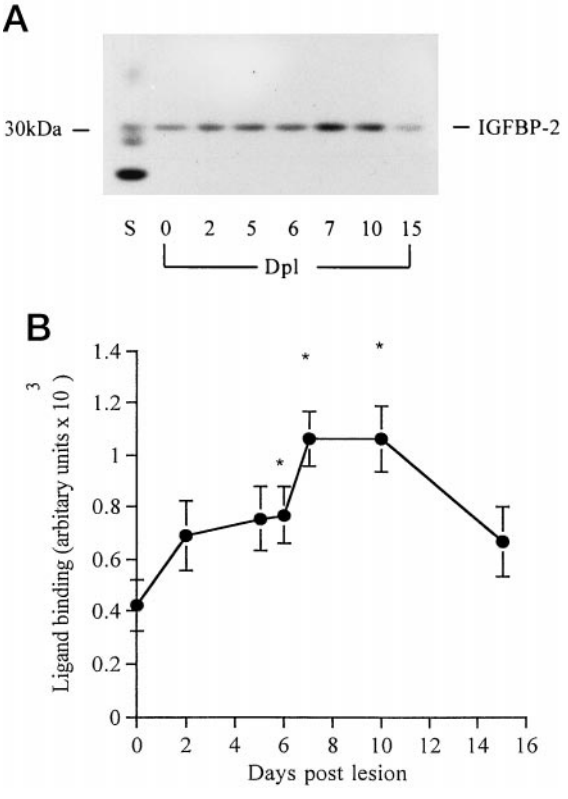

FIG. 6. Western ligand blotting for the determination of the changes in ligand binding to IGFBP-2 within CSF. A, Western ligand blot loaded with a lower volume, 2.5 μl, of the same CSF samples analyzed in Fig. 5, to reveal changes in ligand binding specifically for IGFBP-2; B, relative ligand binding values of the 30 kDa, IGFBP-2 band. Means, SEM, and significance are shown (n = 7). S, Normal serum; Dpl, days post lesion; *, F > Fcrit at the 5% level.

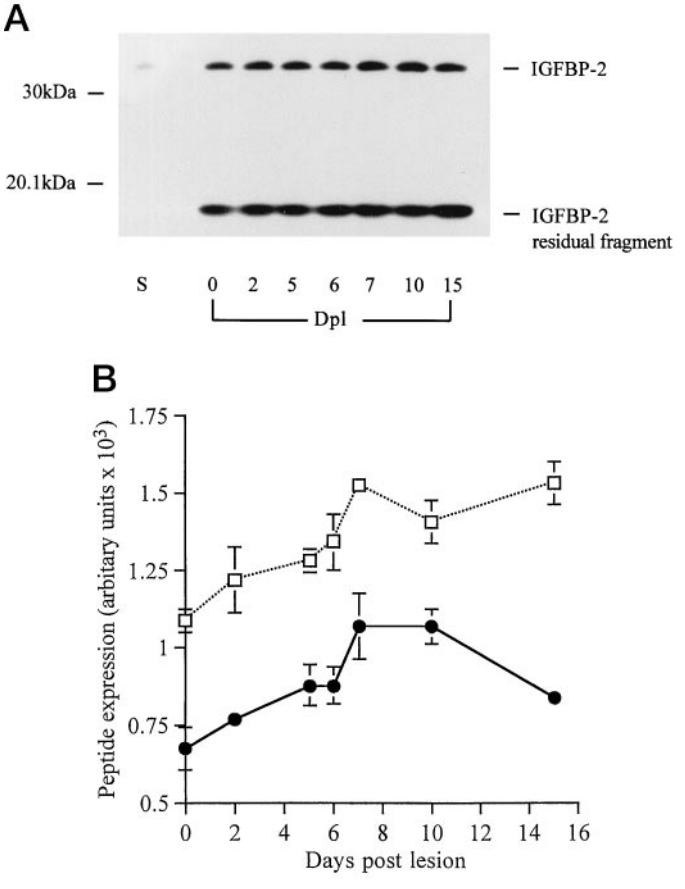

FIG. 7. Western immunoblotting of CSF with anti-IGFBP-2. Immunoblots were performed on Western blots loaded with 2.5 μl sample (n = 2). A, Representative immunoblot; B, relative immunoreactivity values of the 32 kDa and 18 kDa IGFBP-2 bands. Means and SEM are shown (n = 2). S, Normal serum; dpl, days post lesion; ●, 18 kDa, IGFBP-2 residual protein band; □, 32 kDa, IGFBP-2 protein band.

activity is reminiscent of the endocrine delivery of hormones.

This study demonstrates that, despite substantial changes in the IGF-II axis after a penetrating injury to the adult rat brain, the endocrine-like mode of delivery is maintained. Hence, after injury, the bioavailability of IGF-II in wounds is altered, not by local changes in its mRNA expression, but through changes of IGFBP expression and the ensuing import of the IGF-II peptide. Here, we discuss a putative endocrine action of IGF-II in CNS wounds, which differs from

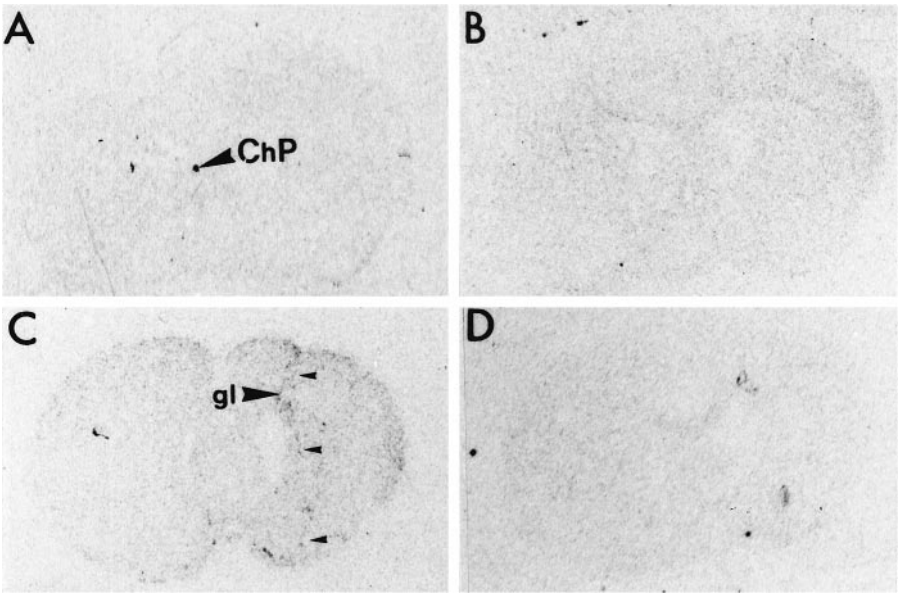

FIG. 8. Autoradiographic macroscopic visualization of IGF-IIR mRNA, by *in situ* hybridization, in brains. A, Intact brain, IGF-IIR antisense hybridized; B, intact brain, IGF-IIR sense hybridized; C, lesioned brain at 12 dpl, IGF-IIR antisense hybridized; D, lesioned brain at 12 dpl, IGF-IIR sense hybridized. ChP, Choroid plexus; gl, glia limitans; *small arrows* depict the lesion path.

the autocrine/paracrine mechanisms previously discussed by us for IGF-I (10).

The acute response of IGF-II, IGFBPs, and IGF-Rs to penetrating CNS injury

In the acute phase response to a penetrating CNS injury (1–7 dpl), IGF-II appears to support the autocrine/paracrine actions of IGF-I in the wound, behaving as a neurotrophin and gliotrophin. The rapid mobilization of IGF-II peptide into the damaged neural parenchyma in the absence of increased local mRNA expression, occurs when cellular activity within the wound is maximal. Therefore, transport for IGF-II, from its site of synthesis in the mesenchymal support structures of the brain to its distal site of action, must occur.

IGF-II, IGFBP-2, IGFBP-3, and IGFBP-6 mRNA are all expressed by the choroid plexi throughout the ventricular system, a likely source of the peptides found within the CSF. The presence of IGF-I peptide was not detected in the CSF, by RIA, in any of the samples taken from unlesioned or lesioned adult rat brains (data not shown; positive control detectable at 0.4 ng/ml). We have detected IGF-II, IGFBP-2, IGFBP-3, and IGFBP-6 peptides within the CSF, with increased levels of each occurring during the acute phase response to injury. However, within the CSF, only IGFBP-2 binds IGF ligands with any significance after injury. With the disruption of the blood-brain barrier that occurs in penetrating wounds, it remains uncertain whether the slightly increased levels of IGFBP-3 and IGFBP-6 are serum derived. From the observed changes in IGFBP titers in the CSF, IGFBP-2 would seem to be the major mediator of IGF-II transport. Within the local parenchyma of the lesion, we have shown that all IGFBPs are present (10) and, therefore, postulate that they are involved in local sequestration and/or modulation of IGF activity within wounds. Interestingly, we have previously shown increased levels of IGFBP-2 mRNA in the wound parenchyma (10), suggesting that additional expression by injury responsive cells may locally regulate IGF actions at this site.

In summary, these studies suggest that there is an acute phase increase in production of IGF-II away from the site of injury by the choroid plexus cells, from where it is transported via the CSF to localize within a CNS wound. Within the CSF, IGF-II is predominately bound by IGFBP-2 and is biologically inert, but changes in the local equilibrium of IGFBPs at the lesion site make it physiologically available to target cells possessing IGF-IR and IGF-IIR including glia and neurons (10). It is possible that IGF-II may also be mobilized both from the myelin sheaths of isolated axons and from myelinated nerve tracts, where the peptide is normally sequestered. Whatever mechanism is implemented, between 3–7 dpl, IGF-II has the potential to function in CNS wounds as a key acute phase endocrine regulator of astrogliosis and neuronal sprouting.

Chronic actions of IGF-II, IGFBPs and IGF-Rs in response to a penetrating CNS injury

During the chronic response to a CNS injury, occurring between 7–15 dpl, IGF-II levels also decline within the CSF, thereby decreasing the supply of bioavailable IGF-II to the wound. Additionally, within the CSF, IGFBP-2 decreases, although the level of the IGFBP-2 18 kDa fragment increases. This fragment, which does not bind IGF-II and may be a product of IGFBP-2 proteolysis within the CSF, may signify attenuation of IGF-II bioactivity.

Within the damaged neural parenchyma of the cerebral wound, the levels of IGF-II and IGFBP-2, -3, and -6 peptides decrease as the wound matures (see also 10). However, at 7 dpl, we observed increasing levels of IGF-II mRNA, colocalized with IGF-II protein, to a specific population of astrocytes bordering the wound. These astrocytes show phenotypic changes as they migrate and secrete matrix components initializing the formation of a glia limitans within the wound, eventually delineating the wound margins to becomes contiguous with the external glia limitans of the brain. The constitutive expression of IGF-II becomes a feature of this selected population of astrocytes, as it is for the astrocytes comprising the glia limitans externa. At this site

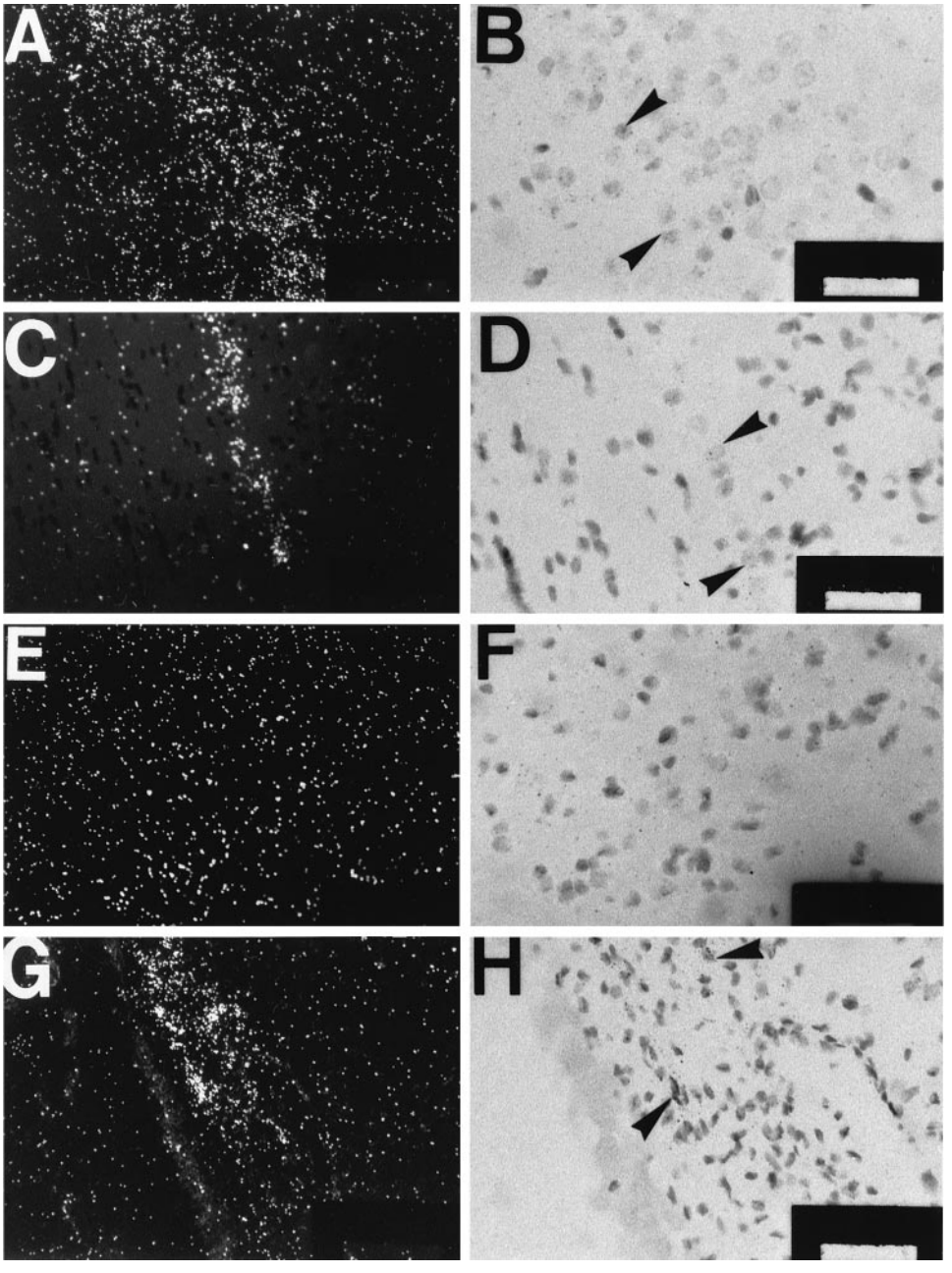

FIG. 9. Microscopic darkfield (DF) and brightfield (BF) visualization of IGF-IIR mRNA, by *in situ* hybridization, in brains. *Arrows* indicate sites of positive hybridization. A, Piriform cortex, intact brain (DF); B, piriform cortex, intact brain (BF); C, internal capsule, intact brain (DF); D, internal capsule, intact brain (BF); E, unlesioned cerebral cortex at 12 dpl (DF); F, unlesioned cerebral cortex at 12 dpl (BF); G, lesioned cerebral cortex at 12 dpl, taken from the neuropil surrounding the lesion path (DF); H, lesioned cerebral cortex at 12 dpl, taken from the neuropil surrounding the lesion path (BF). *Bar*, 10 μm (DF) and 5 μm (BF).

and elsewhere in the intact and lesioned brain we have shown that the constitutive expression of IGF-II and IGFBP-2 are spatially and temporally coincident (4).

The levels of IGF-IR mRNA expression remain unaltered in response to a penetrating injury to the CNS (10), suggesting that changes in IGF-IR expression are not a primary determinant of IGF bioactivity. We presume that increased IGF-IIR levels in injury responsive astrocytes and neurons in the acute wound (2–5 dpl) derive from distant sites of synthesis because no corresponding mRNA was detectable. Although a soluble form of the IGF-IIR peptide has been identified in a variety of serum sources (47, 48), we were unable to detect its presence within the CSF, by Western blotting, in samples taken from unlesioned and lesioned adult rat brains (data not shown). However, during the chronic response to injury (after 12 dpl), IGF-IIR mRNA expression did increase focally with IGF-II mRNA within selected astrocytes comprising the maturing glia limitans of the scar in a similar manner to that of IGF-II and IGFBP-2. Interestingly, increased expression of IGFBP-5 mRNA has also been demonstrated in the reforming glia limitans of the injured brain at the same time (10). IGFBP-5 reportedly inhibits IGF in many tissue systems (9) and may assist in the sequestration of IGF-II in the wound during the later phase of the injury response, thereby modulating IGF-II activity at this site. The highly coordinated expression of these interacting proteins in the chronic CNS lesion implicates a role for these factors in the reestablishment and maintenance of the integrity of the glia limitans. Therefore, in the chronic phase of the CNS wounding response, IGF-II may reassert its actions as an

autocrine/paracrine factor within the glia limitans of the wound, in contrast to the acute phase endocrine action seen locally in the neural parenchyma.

In summary, a second mechanism for IGF-II action in the chronic phase of CNS injury is proposed. In the intact brain, constitutive IGF-II and IGFBP-2 mRNA and protein expression are a phenotypic feature of the astrocytes present within the glia limitans externa. It is possible that their role is to maintain homeostasis in the mesenchymal support structures of the brain, primarily by an autocrine/paracrine mechanism. In the chronic phase response to injury, after the endocrine-like acute phase response in the wound neuropil, we postulate that IGF-II reverts to its primary role as an autocrine/paracrine factor in the maturing glial membranes of the wound. Hence, at this time, levels of IGF-II mRNA increase to constitutive levels focally in the differentiating astrocytes of the wound glia limitans thereby helping to restore tissue homeostasis.

In conclusion, we propose that within the uninjured brain IGF-II expression in the mesenchymal support structures is associated with an autocrine/paracrine role in tissue homeostasis. IGF-II and IGFBP-2 mRNA are constitutively expressed by the choroid plexus throughout the brain. The presence of immunoreactive IGF-II within the CSF and localization within myelinated tracts under normal physiology suggests circulation within the former and sequestration at the latter distal depots; a pattern of transport and deposition which is maintained after injury. After a penetrating CNS injury, this pattern of expression is maintained with IGF-II synthesized at sites distal to its sites of bioactivity. During the acute phase of the wounding response, IGF-II expression is up-regulated in the choroid plexus cells, which leads to the increased secretion of the peptide into the CSF. Consequentially, there is an increase in transportation to the wound of IGF-II complexed to IGFBP-2, where it may target receptor-bearing glia and neurons. Hence, an essentially endocrine mode of action is indicated for IGF-II during the early phases of CNS wounding, with a balance of locally produced stimulatory/inhibitory IGFBPs modulating its bioactivity. Later in the response, as the IGF-II levels drop in the neural parenchyma around the wound, IGF-II may reassert its autocrine/paracrine role in the maintenance of tissue homeostasis via actions at the glial membrane.

Acknowledgments

Our thanks are due to Fiona Ruge and Jonathan Carlisle for their assistance in sectioning tissue samples.

References

1. **Logan A, Oliver JJ, Berry M** 1995 Growth factors in CNS repair and regeneration. Prog Growth Factor Res 5:379–405
2. **Berry M, Butt A, Logan A** 1998 Cellular responses to penetrating CNS injury. In: Berry M, Logan A (eds) Monograph: Therapeutic Strategies in the Treatment of CNS Injury. CRC Press Inc., Boco Raton, FL, pp 1–18
3. **McKelvie PA, Rosen KM, Kinney HC, Villa-Komaroff L** 1992 Insulin-like growth factor II expression in the developing human brain. J Neuropathol Exp Neurol 51:464–471
4. **Logan A, Gonzalez A-M, Hill DJ, Berry M, Baird A** 1994 Co-ordinated pattern of expression and localization of insulin-like growth factor (IGF)-II and IGF binding protein-2 in the adult rat brain. Endocrinology 135:2255–2264
5. **Ayer-le-Lievre C, Stahlbom PA, Sara VR** 1991 Expression of IGF-I and -II mRNA in the brain and craniofacial region of the rat fetus. Development 111:105–115
6. **Berry MM, Standring SM, Bannister LH** 1997 Fluid compartments and fluid balance in the CNS. In: Williams PL, Bannister LH, Berry M, Collins P, Dyson M, Dusek JE, Ferguson MW (eds) Gray's Anatomy. Churchill Livingstone, Edinburgh, pp 1202–1224
7. **Hasselbacher G, Humbel R** 1982 Evidence for two species of insulin-like growth factor II (IGFII and "big" IGFII) in human spinal fluid. Endocrinology 110:1822–1824
8. **Clemmons DR** 1997 Insulin-like growth factor binding proteins and their role in controlling IGF actions. Cytokine Growth Factor Rev 8:45–62
9. **Jones JI, Clemmons DR** 1995 Insulin-like growth factors and their binding proteins: biological actions. Endocr Rev 16:3–24
10. **Walter HJ, Berry M, Hill DJ, Logan A** 1997 Spatial and temporal changes in the insulin-like growth factor (IGF) axis indicate autocrine/paracrine actions of IGF-I within wounds of the rat brain. Endocrinology 138:3024–3034
11. **Stenvers KL, Zimmermann EM, Gallagher M, Lund PK** 1994 Expression of insulin-like growth factor binding protein-4 and -5 mRNAs in adult rat forebrain. J Comp Neurol 339:91–105
12. **Brar AK, Chernausek SD** 1993 Localization of insulin-like growth factor binding protein-4 expression in the developing and adult rat brain: analysis by hybridization. J Neurosci Res 35:103–114
13. **Delhanty PJD, Hill DJ, Shimasaki S, Han VKM** 1993 Insulin-like growth factor binding protein-4, protein-5 and protein-6 messenger RNAs in the human fetus-localization to sites of growth and differentiation. Growth Regul 3:8–11
14. **Shimasaki S, Gao L, Shimonaka M, Ling N** 1991 Isolation and molecular cloning of insulin-like growth factor binding protein-6. Mol Endocrinol 5:938–948
15. **Ocrant I** 1993 Insulin-like growth factor binding proteins in nervous-tissue derived cells. Ann NY Acad Sci 692:44–50
16. **Müller HL, Oh Y, Lehrnbecher T, Blum WF, Rosenfeld RG** 1994 Insulin-like growth factor-binding protein-2 concentrations in cerebrospinal fluid and serum of children with malignant solid tumors or acute leukemia. J Clin Endocrinol Metab 79:428–434
17. **Gargosky SE, Pham HM, Wilson KF, Liu F, Giudice LC, Rosenfeld RG** 1992 Measurement and characterization of insulin-like growth factor binding protein-3 in human biological fluids: discrepancies between radioimmunoassay and ligand blotting. Endocrinology 131:3051–3060
18. **Ocrant I, Fay CT, Parmelee JT** 1990 Characterization of insulin-like growth factor binding proteins produced in the rat central nervous system. Endocrinology 127:1260–1267
19. **Roghani M, Hossenlopp P, Lepage P, Balland A, Binoux M** 1989 Isolation from human cerebrospinal fluid of a new insulin-like growth factor-binding protein with a selective affinity for IGF-II. FEBS Lett 255:253–258
20. **Kar S, Chabot J-G, Quiron R** 1993 Quantitative autoradiographic localization of [^{125}I]insulin-like growth factor I, [^{125}I]insulin-like growth factor II, and [^{125}I]insulin receptor binding sites in developing and adult rat brain. J Comp Neurol 333:375–397
21. **Girbau M, Bassas L, Alemany J, De Pablo F** 1989 *In situ* autoradiography and ligand-dependent tyrosine kinase activity reveal insulin receptors and insulin-like growth factor receptors in pancreatic chicken embryos. Proc Natl Acad Sci USA 86:5868–5872
22. **Werner H, Woloschek M, Adamo M, Shen-Orr Z, Roberts CTJ, LeRoith D** 1989 Developmental regulation of the rat IGF-I receptor gene. Proc Natl Acad Sci USA 86:7451–7455
23. **Ocrant I, Valentino KL, Eng LF, Hintz RL, Wilson DM, Rosenfeld RG** 1988 Structural and immunohistochemical characterization of insulin-like growth factor I and II receptors in the murine central nervous system. Endocrinology 123:1023–1034
24. **De Keyser J, Wilczak N, De Backer J-P, Herroelen L, Vauquelin G** 1994 Insulin-like growth factor-I receptors in human brain and pituitary gland: an autoradiographic study. Synapse 17:196–202
25. **Werther GA, Hogg A, Oldfield BJ, McKinley MJ, Figdor R, Mendelson FAO** 1989 Localization and characterization of IGF-I receptors in rat brain and pituitary gland using *in vitro* autoradiography and computerized densitometry: a distinct distribution from insulin receptors. J Neuroendocrinol 1:369–377
26. **Bohannon NJ, Corp ES, Wilcox BJ, Figlewicz DP, Dorsa DM, Baskin DG** 1988 Localization of binding sites for insulin-like growth factor-I (IGF-I) in the rat brain by quantitative autoradiography. Brain Res 444:205–213
27. **Lesniak MA, Hill JM, Kiess W, Rojeski M, Pert CB, Roth J** 1988 Receptors for insulin-like growth factors I and II: autoradiographic localization in rat brain and comparison to receptors for insulin. Endocrinology 123:2089–2099
28. **Reinhardt RR, Bondy CA** 1994 Insulin-like growth factors cross the blood-brain barrier. Endocrinology 135:1753–1761
29. **Kiess W, Haskell JF, Lee L, Greenstein LA, Miller BE, Aarons AL, Rechler MM, Nissley SP** 1987 An antibody that blocks insulin-like growth factor (IGF) binding to the type II IGF receptor is neither an agonist nor an inhibitor of IGF-stimulated biologic responses in L6 myoblasts. J Biol Chem 262:12745–12751
30. **Conover CA, Misra P, Hintz RL, Rosenfeld RG** 1986 Effect of an anti-insulin-like growth factor I receptor antibody on insulin-like growth factor II stimu-

lation of DNA synthesis in human fibroblasts. Biochem Biophys Res Commun 139:501–508
31. **Rogers SA, Hammerman MR** 1988 Insulin-like growth factor II stimulates production of inositol triphosphate in proximal tubular basolateral membranes from canine kidney. Proc Natl Acad Sci USA 85:4037–4041
32. **Nishimoto I, Hata Y, Ogata E, Kojima I** 1987 Insulin-like growth factor II stimulates calcium influx in competent BALB/c 3T3 cells primed with epidermal growth factor. Characteristics of calcium influx and involvement of GTP-binding protein. J Biol Chem 262:12120–12126
33. **Rotwein P, Burgess SK, Milbrandt JD, Krause JE** 1988 Differential expression of insulin-like growth factor genes in rat central nervous system. Proc Natl Acad Sci USA 85:4904–4907
34. **Couce ME, Weatherington AJ, McGinty JF** 1992 Expression of insulin-like growth factor-II (IGF-II) and IGF-II/mannose-6-phosphate receptor in the rat hippocampus: an *in situ* hybridization and immunocytochemical study. Endocrinology 131:1636–1642
35. **Hill JM, Lesniak MA, Kiess W, Nissley SP** 1988 Radioimmunohistochemical localization of type II IGF receptors in rat brain. Peptides 9:181–187
36. **Valentino KM, Pham H, Ocrant I, Rosenfeld RG** 1988 Distribution of insulin-like growth factor II receptor immunoreactivity in rat tissues. Endocrinology 122:2753–2763
37. **Caroni P, Grandes P** 1990 Nerve sprouting in innervated adult skeletal muscle induced by exposure to elevated levels of insulin-like growth factors. J Cell Biol 110:1307–1317
38. **Knüsel B, Michel PP, Schwaber JS, Hefti F** 1990 Selective and nonselective stimulation of central cholinergic and dopaminergic development *in vitro* by nerve growth factor, basic fibroblast growth factor, epidermal growth factor, insulin and the insulin-like growth factors I and II. J Neurosci 10:558–570
39. **Hill DJ, Han VK** 1991 Paracrinology of growth regulation. J Dev Physiol 15:91–104
40. **Steedman HF** 1957 A new ribboning embedding medium for histology. Nature 197:1345
41. **Chomcyznski S, Sacchi N** 1987 Single-step method of RNA isolation by guanidinium thiocyanate-phenol-chloroform extraction. Anal Biochem 162:156–159
42. **Ausubel FM, Brent R, Kingston RE, Moore DD, Smith JA, Struhl K** 1992 Short Protocols in Molecular Biology, ed 2. John Wiley & Sons, Chichester
43. **Hill DJ** 1990 Relative abundance and molecular size of immunoreactive insulin-like growth factors I and II in human fetal tissues. Early Human Dev 21:49–58
44. **Nilsson C, Lindvall-Axelsson M, Owman C** 1992 Neuroendocrine regulatory mechanisms in the choroid plexus-cerebrospinal fluid system. Brain Res Brain Res Rev 17:109–138
45. **Tseng LY-H, Brown AL, Yang W-H, Romanus JA, Orlowski CC, Taylor T, Rechler MM** 1989 The fetal rat binding protein for insulin-like growth factors is expressed in the choroid plexus and cerebrospinal fluid of adult rats. Mol Endocrinol 3:1559–1568
46. **Hossenlopp P, Seurin D, Segovia-Quinson B, Binoux M** 1986 Identification of an insulin-like growth factor-binding protein in human cerebrospinal fluid with a selective affinity for IGF-II. FEBS Lett 208:439–444
47. **Causin C, Waheed A, Braulke T, Junghans U, Maly P, von Figura K** 1988 Mannose-6-phosphate/insulin-like growth factor II-binding proteins in human serum and urine. Their relation to the mannose-6-phosphate/insulin-like growth factor II receptor. Biochem J 252:795–799
48. **Kiess W, Greenstein LA, White RM, Lee L, Rechler MM, Nissley SP** 1987 Type II insulin-like growth factor receptor is present in rat serum. Proc Natl Acad Sci USA 84:7720–7724